DEVELOPMENT OF THE FOREST FIRE DETECTION ALGORITHM FOR GCOM-C1/SGLI

Takashi Miura, Masao Moriyama

1-14 Bukyo-machi Nagasaki Japan
Telephone: 81-95-819-2579 FAX: 81-95-819-2575
E-mail address: nova@rsirc.cis.nagasaki-u.ac.jp

Commission VIII/8

KEY WORDS: Fire monitoring, Fire mixed pixel, Characteristics of fire pixel, Fixed threshold, Contextual threshld, Detection limit

ABSTRACT:

This paper presents a development of the forest fire detection algorithm for upcoming GCOM-C1/SGLI sensor. Several existing fire detection algorithms which are applied to GOES/VAS, NOAA/AHVRR, Terra Aqua/MODIS sensors mainly use the MIR fire channels(3-4μm) for key role of the fire detection algorithm. Meanwhile, because of lack of the MIR fire channel on GCOM-C1/SGLI, fire detection algorithm must be developed using general land/atmosphere observation channels. For this reason, we investigated the significant channels for the fire detection process and determined the frameworks of the fire detection algorithm for SGLI. The proposed fire detection algorithm mainly uses the second principal component score of SWIR 1.6μm and 2.2μm channel's radiance, and the second principal component score of NIR 0.8μm and SWIR 1.6μm channel's radiance to detect fire pixels. The algorithm is organized with complex of the various threshold tests. Comparison between the fire detection result on this algorithm and ASTER fire detection result under 30m high resolution data using an automated fire detection algorithm for ASTER(Giglio et al., 2008) shows that the detection accuracy of this algorithm is 14% of producer's accuracy and 87% of user's accuracy and fire pixels which has a fire fraction over 2.5% or a fire temperature over 1000[K] can be detected using developed algorithm.

1 INTRODUCTION

Wild fire is one of the process which affects on the regional and global climate system. For this reason, wlid fire monitoring is important to understand a part of mechanism of the climate changes. Recently, wild fire monitoring activeties are carried out using the remotely sensed data of several existing satellite sensors that are for example Terra/MODIS, NOAA/AVHRR. GCOM which is a mission of JAXA to investigate the mechanism of the global climate change using the series of satellites (GCOM-WX, GCOM-CX) has been planed and the wild fire monitoring activity using upcoming GCOM-C1/SGLI sensor will be also carried out as the one of the task of GCOM mission. The fire detection process is a part of the wild fire monitoring activety. Wild fire detection results give the information of the location of fire occurrences. The fire detection algorithms which are applied to exsiting sensors such as MODIS mainly use the MIR 4-μm fire channel which is the most sensitive to the high temperature objects such as wild fires. For this reason, fire channel is the most significant to the fire detection process. Meanwhile, because of the lack of the MIR fire channel on SGLI, fire detection algorithm for SGLI must be developed using only general surface observation channels. For this reason, we need to develop the fire detection algorithm for SGLI and determine the frameworks of the algorithm in this paper.

2 FIRE DETECTION

2.1 Data

ASTER instrument has the bands are the similar to that of SGLI, so that we used remotely sensed 26 fire scenes which are aquired from ASTER as imitative SGLI data for this paper. The ASTER Level 1B calibrated radiance data was used for the fire detection algorithm development in this paper. ASTER images are averaged to corser SGLI resolution using aggregation to imitate SGLI image. The locations of the fire scenes are shown in Figure 1.

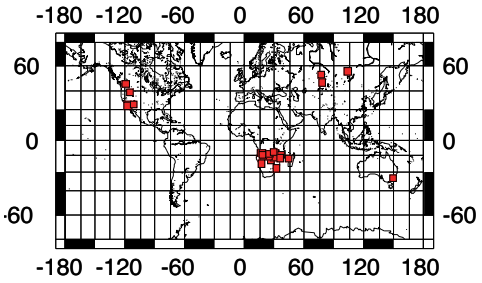

Figure 1: Locations of the ASTER fire scenes used in this study.

2.2 Band selection

Table 1 shows the specifications of SGLI bands which are available for the fire detection process. First, we performed the sensitive analysis with the simulation to show that which bands of SGLI are more sensitive to the fires. The radiance of the pixel which is contaminated with the high temperature object such as fire is shown as below.

Table 1: SGLI specification

Center wavelength	Spatial resolution
0.8μm	250 m
1.6μm	250 m
2.2μm	1000 m
10.8μm	500 m

$$I_\lambda = pB_\lambda(T_f) + (1-p)B_\lambda(T_b) \quad (1)$$

Where, T_f is fire temperature, T_b is the background land surface temperature, p is the fraction of the fire area per one pixel, $B_\lambda(T)$

is the Planck function at the temperature T and the wavelength λ. Second, on the basis of this mixed pixel model, we evaluated the the defference of radiance between fire contaminated pixel ($I_{f\lambda}$) and non-contaminated pixel ($I_{b\lambda}$) as the sensitivety to the fire which is shown as below.

$$\begin{aligned} \Delta I_\lambda &= I_{f\lambda} - I_{b\lambda} \\ &= [pB_\lambda(T_f) + (1-p)B_\lambda(T_b)] - B_\lambda(T_b) \end{aligned} \quad (2)$$

This simulation is performed on the condition that p is 0.0001 - 1, T_f is 600[K] and 1200[K], T_b is 300[K] and solar reflections and atmospheric effect were ignored. Figre.2 shows the result of the sensitivety analysis. In the case where T_f = 600[K], 2.2μm is sensitive to the fire and then the fire temperature comes to more higher i.e. T_f = 1200[K], 1.6μm is also sensitive to the fire. Taking into account the result of the sensitive analysis with the simulation, we employ 1.6μm and 2.2μm as the main bands of the SGLI fire detection algorithm.

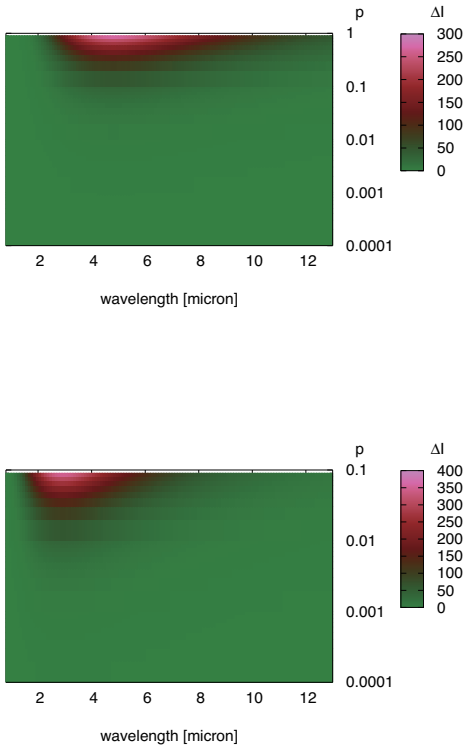

Figure 2: Result of sensivety analysis to the fire. Top:$T_f = 600[K]$ Bottom:$T_f = 1000[K]$

2.3 Fire detection algorithm

Next, we determined the framework of the fire detection algorithm for SGLI in this section. To organize the fire detection algorithm, we investigated the charasteristics of the fire pixel for the detection process. First, we simulated the satellite-level radiance of several land surface components using 6S (Second Simulation of a Satellite Signal in the Solar Spectrum vector code) The simulation conditions which were inputed into 6S are shown as below.

- solar zenith: 80°, 70°, 60°, 50°, 40°, 30°, 20°
- solar azimth: 157.5°
- sensor view angle: Nadir
- atomospheric condition: U.S.62
- aerosol model: Biomass burning model
- visibility: 5[km]
- sensor chs.:
  - ASTER band3N (0.8μm)
  - ASTER band4 (1.6μm)
  - ASTER band7 (2.2μm)
- land surface components:
  - VEGETATION
  - SAND
  - CLEAR WATER
  - LAKE WATER

On this simulation using 6S, the radiance of the land surface components and the upwelling atmospheric transmittance can be retrieved. Second, the simulated radiance of VEGETATION which is denoted by L_λ^{VEG} and the upwelling atmospheric trancemittance which is denoted by $\tau_\lambda^{\uparrow}$ are inputted into the fire mixed pixel model shown as below.

$$I_\lambda = \tau_\lambda^{\uparrow} pB_\lambda(T_f) + (1-p)L_\lambda^{VEG} \quad (3)$$

The results of the simulated I_λ with eq.(3) are shown in Figure 3. Figure 3 shows that the distribution of general land components

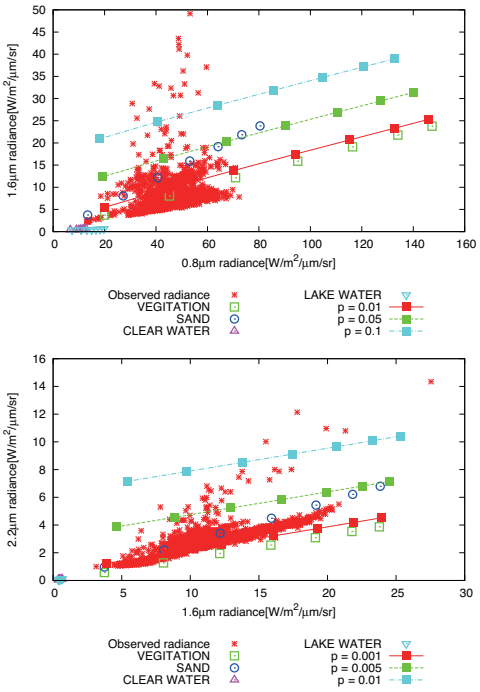

Figure 3: Simulation result of the fire mixed pixels. Top:0.8μm vs 1.6μm Bottom:1.6μm vs 2.2μm

scatter toward the uniform direction as the solar zenith angle vary from 20° to 80°. Meanwhile, the distribution of the fire mixed pixels tend to extend vertically against the direction of the distribution of genelal land components as the fire scale grows. This result means that the influence of the sun glint, which accounts for the false alarm occurs in the fire detection process, is confined to the direction of the first principal component which is denoted by $PC1$, and the effect of the fire appears toward the direction of the second principal component denoted by $PC2$. Figure 4. shows the scatter plot of $PC1$ and $PC2$. Taking into account of the result of this simulation, we employ $PC2$ score of 0.8μm and 1.6μm radiance under 250m spatial resolution which is denoted by $PC2^{250m}$ and 1.6μm and 2.2μm radiance under 1000m spatial resolution which is denoted by $PC2^{1000m}$ as the main charasteristic for the SGLI fire detection algorithm. And we also refer to the ratio of radiances to detect fires. Using radiances of 0.8μm, 1.6μm, 2.2μm, denoted by $L_{0.8\mu m}$, $L_{1.6\mu m}$ and $L_{2.2\mu m}$ respectively, we calculate the ratio of radiances, where $R^{250m} = L_{0.8\mu m}/L_{1.6\mu m}$ and $R^{1000m} = L_{1.6\mu m}/L_{2.2\mu m}$.

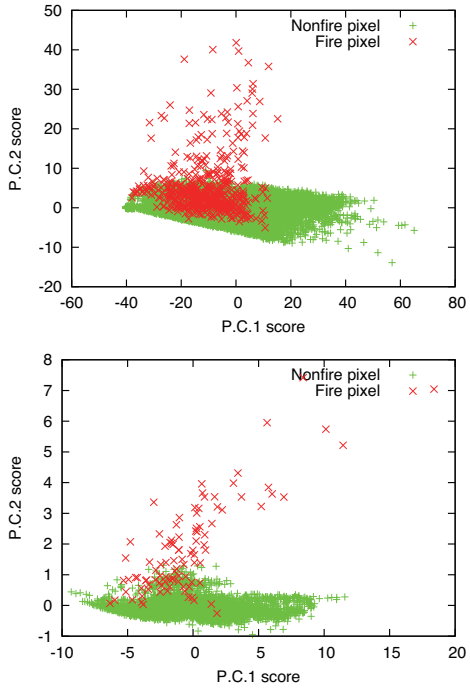

Figure 4: PC1 score vs PC2 score. Top:PC scores of 0.8μm and 1.6μm Bottom:PC scores of 1.6μm and 2.2μm

First, $PC2$ score is calculated from data population on an each observed scene which is as wide as ASTER scene and the calculated $PC2$ score image is used for the fire detection algorithm. Second, fixed threshold tests are performed to detect obvious fire pixel. In order to prevent the occurrence of false alarms, fixed threshold values are set high. The conditions of the fixed threshold test are shown as below.

$$PC2^{1000m} > 2.0 \quad (4)$$
$$or$$
$$PC2^{250m} > 11.0 \quad and \quad R^{250m} > 0.4$$

Next, contextual threshold tests are performed to detect fire pixels which cannot be detected on the fixed threshold tests. On the contextual threshold test, arithmetic mean of $PC2$ which is denoted by $\bar{PC2}$ and standard deviation of $PC2$ which is denoted by σ_{PC2} are caluculated within 21x21 moving window. Fire pixels which are detected by previous threshold tests are eliminated when these statistics are calculated. Then the center pixel of the window is compared to the caluculated statistics($\bar{PC2}$, σ_{PC2}). The conditions of the fixed threshold test are shown as below.

Contextual test under 1000m

$$PC2^{1000m} > \bar{PC2^{1000m}} + 6.0\sigma_{PC2^{1000m}} \quad (5)$$
$$and$$
$$R^{1000m} > 0.25$$
$$or$$
$$PC2^{1000m} > \bar{PC2^{1000m}} + 4.0\sigma_{PC2^{1000m}}$$
$$and$$
$$R^{1000m} > 0.32$$

Contextual test under 250m

$$PC2^{250m} > \bar{PC2^{250m}} + 4.5\sigma_{PC2^{250m}} \quad (6)$$
$$and$$
$$R^{250m} > 0.33$$
$$or$$
$$PC2^{250m} > \bar{PC2^{250m}} + 4.0\sigma_{PC2^{250m}}$$
$$and$$
$$R^{250m} > 0.39$$
$$or$$
$$PC2^{250m} > \bar{PC2^{250m}} + 3.5\sigma_{PC2^{250m}}$$
$$and$$
$$R^{250m} > 0.43$$

3 ACCURACY ASSESSMENT

3.1 Detection result and detection accuracy

3.1.1 Truth fire mask Giglio et al.(2) developped an automated fire detection algorithm for ASTER 30m high resolution data. This algorihm is well assessed in their paper and has adequete accuracy as fire truth data for the moderate resolution data. So we employ the result of Giglio's fire detection algorithm as the truth fire data.

3.1.2 Fire detection result Detection result images of developped algorithm are shown in Figure 5. Figure 5. shows that large and bright fires can be detected and small fires which remain undetected under fixed threshold test could be detected with this algorithm.

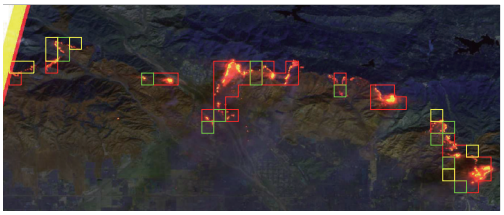

Figure 5: Fire detection result. Red:Fixed test Green:Contextual test under 1000m resolution Yellow:Contextual test under 250m resolution

3.1.3 Fire detection accuracy For each evaluation scene, fire detection result of Gilgio's algorithm were considered as expart

truth fire mask. And then these masks were compared to detection result of developed algorithm. To evaluate the detection accuracy, User's accuracy and Producer's accuracy are considered in the assessment of the detection accuracy.

		Detection result		
		Fire	Non fire	Total
ASTER fire mask	Fire	225	1412	1637
	Non fire	34	103787	
	Total	259		

User's accuracy = 225/259 = 87 [%]
Producer's accuracy = 225/1637 = 14 [%]

Table 2: Detection accuracy.

Fire detection result is shown in Table 2. User's accuracy is 87% and Producer's accuracy is 14% by comparison with ASTER 30m fire mask. High user's accuracy means that detection result on this algorithm has high reliability. Meanwhile, many small fire crusters and thin fire front line which remain undetected cause low producer's accuracy.

3.2 Validation with simulation

3.2.1 Method Simulated radiance images were generated using original ASTER fire scenes. Fire pixels in the original ASTER image were replaced with idealized fire pixels of various size and temperatures which were set manually. The idealized fire fraction of the pixel in this simulation is generated as Figure 6. First, number of ASTER 30m fire pixels within 1000m resolution pixel which is denoted by N and number of the 30m resolution pixels within 1000m resolution pixel which is denoted by S are counted. The idealized fire fraction under 1000m resolution which is denoted by p_{1000} is assigned with random numbers under the condition shown as below.

$$0 < p_{1000} \leq \frac{N}{S} \tag{7}$$

Second, number of ASTER 30m fire pixels within 250m resolution which is denoted by n_i is counted. And then number of the 30m resolution pixels within 250m resolution pixel which is denoted by s_i are counted. Where, i is identification number of 250m pixel within 1000m pixel. The idealized fire fraction under 250m resolution which is denoted by p^i_{250} is assigned as below.

$$p^i_{250} = \frac{p_{1000} S \frac{n_i}{N}}{s_i} \tag{8}$$

The idealized fire temperature which is denoted by T_f is assigned by drawing random samples from normal distributions that is described as below.

$$T_f \sim N(800.0[K], 100[K]) \tag{9}$$

The background land surface radiance of the fire pixel which is denoted by L^{BKG}_{λ} is estimated from average of neighboring pixels which are within 21x21 window. The upwelling transmittance $\tau^{\uparrow}_{\lambda}$ is simulated using 6S. Finally, the idealized fire pixel is simulated using fire mixed pixel model shown as eq.(3) and then the fire detection algorithm is applied to the synthetic fire scenes.

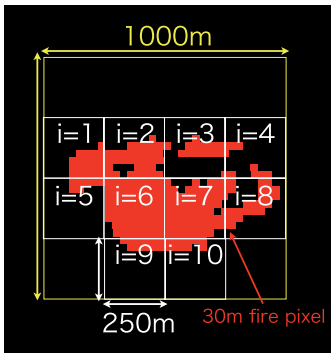

Figure 6: Characterize of the idealized fire fraction

3.2.2 Result Simulated fire detection result is shown in Figure 7. When the fire temperature is high i.e. 1000[K]∼, fire pixels which has the fire fraction of 0.0005 can be almost detected. And when fire temperature is moderate i.e 800[K], fire pixels which has the the fire fraction of 0.0025 could be detected. And when fire temperature is low i.e 600[K], fire pixels which has the the fire fraction of 0.025 could be detected.

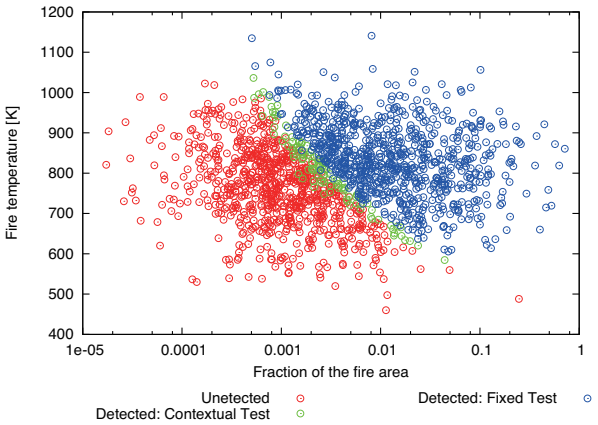

Figure 7: Simulated detection result

4 CONCLUSIONS

We have described the fire detection algorithm for SGLI. The second principal components score of NIR and SWIR bands is significant to detect fires. Higher 250m resolution bands have an advantage of detection of small fires which remain undetected under 1000m resolution case. A large number of small fires and thin fire front lines remain undetected and false alarms almost exist at burn scar and bright objects, and some clouds and water pixels are also detected as false alarm on this algorithm.

REFERENCES

(1)Giglio, L., Descloitres, J., Justice, C., O., Kaufman, Y., J., 2003, An enhanced contextual fire detection algorithm for MODIS. *Remote Sensing of Environment*, **87**, 273-282

(2)Giglio, L., Csiszar, I., Ágoston Testás, Morisette, J., T., Schroeder, W., Morton, D., Justice, C., O., 2008, Active fire detection and characterization with the advanced spaceborne thermal emission and reflection radiometer(ASTER). *Remote Sensing of Environment*, **112**, 3055-3063